PHYSICAL REVIEW E **68**, 060702(R) (2003)

Unusual behavior of the surface-induced tilted layers in free-standing films of a non-layer-shrinkage liquid crystal compound

S. T. Wang,[1] X. F. Han,[1] Z. Q. Liu,[1] A. Cady,[1,*] M. D. Radcliffe,[2] and C. C. Huang[1]
[1]*School of Physics and Astronomy, University of Minnesota, Minneapolis, Minnesota 55455, USA*
[2]*3M Company, St. Paul, Minnesota 55144, USA*
(Received 12 September 2003; published 23 December 2003)

Null-transmission ellipsometry has been conducted to study the molecular arrangements in free-standing films of one chiral compound above the bulk smectic-*A*–smectic-*C** transition temperature. Upon cooling under a proper electric field, a nonplanar-anticlinic-synclinic or a nonplanar-synclinic transition has been observed. The nonplanar structure continuously evolves into the anticlinic or synclinic structures. Increasing electric field can induce a rare transition from a synclinic to an anticlinic structure.

DOI: 10.1103/PhysRevE.68.060702 PACS number(s): 61.30.Eb, 77.84.Nh

In recent years, non-layer-shrinkage (NLS) liquid crystals have gained enormous interest in both basic science and technological applications [1–4]. In addition to the lack of layer contraction at the smectic-*A*–smectic-*C* (Sm-*A*–Sm-*C*) transition, this class of compounds usually shows anomalous electroclinic effect and low birefringence [5,6]. By employing these unique physical properties, new electro-optical switching devices have been designed, including potentially the fastest switching liquid-crystal displays with gray scale. To date, most of the experimental data have been qualitatively explained by the de Vries diffuse-cone model [7]. In the conventional Sm-*A* phase, all molecules have their long axes approximately parallel to the layer normal. From the measured nematic order parameter in the Sm-*A* phase, de Vries argued that the molecules are significantly tilted in each layer. The azimuthal disorder yields the uniaxial Sm-*A* phase. To date, the diffuse-cone model provides a good starting point and qualitative description of some physical properties among the NLS liquid crystals. In light of obviously systematic deviation between the experimental data and the theory derived from such a model [6], another microscopic theory has been proposed recently by Meyer and Pelcovits [8]. To date, numerous questions related to the NLS liquid crystals remain to be answered.

Free-standing films with quantized thickness have played an important role in elucidating the phase behavior and molecular arrangements of bulk samples [9–12]. Due to the enhanced ordering of the surface layers, there exists a reasonably wide temperature window in which rich surface phases can be studied [13,14]. Previous experiments have demonstrated that the surface-induced tilted layers on two free surfaces can tilt in the same orientation (synclinic) [15–17] or in the opposite orientation (anticlinic) [18–20]. Some remarkable results have also been found from the free-standing films of NLS compounds. The nonplanar surface structure was first observed in one of this type of compounds under a small electric field [21]. Recent studies on one of NLS compounds with a fluoroether tail have yielded a double reentrant transition between synclinic and anticlinic surface structures [22]. Here we will report another unusual behavior produced by the surface-induced tilted layers from another fluoro-containing compound.

We conducted detailed experimental studies of 8O23[7F8-] which displays NLS. Its molecular structure is given in Fig. 1. The transition sequence is isotropic $\overleftrightarrow{95.5}$ °C Sm-*A* $\overleftrightarrow{79.9}$ °C Sm-*C** $-\overleftrightarrow{12.1}$ °C crystal. Our result shows a nonplanar-anticlinic-synclinic or nonplanar-synclinic transition upon cooling depending on the strength of applied electric field *E*. The nonplanar-anticlinic and nonplanar-synclinic transitions are found to be continuous. A field induced transition from synclinic to anticlinic state is observed upon increasing *E*.

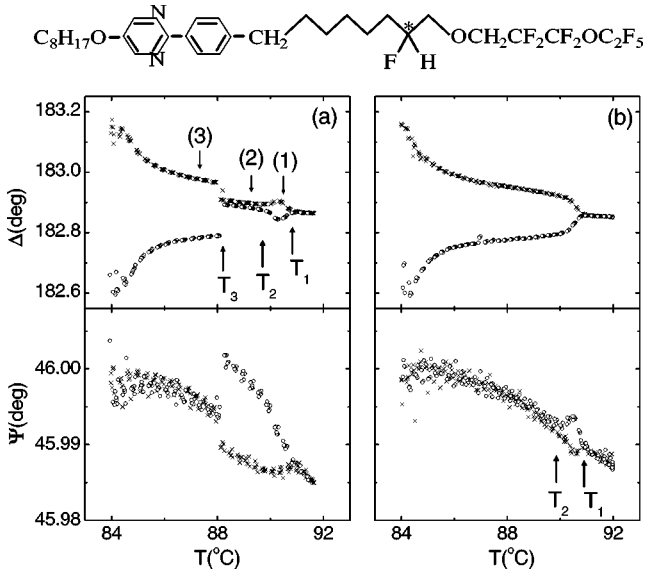

FIG. 1. Temperature dependence of Δ and Ψ obtained upon cooling under two opposite directions of *E* from a ten-layer film with (a) $E=22$ V/cm and (b) $E=8.9$ V/cm. Crosses and open circles are data obtained under $\alpha=90°$ and $\alpha=270°$, respectively. In (a), three upward arrows located at $T_1=90.8$ °C, $T_2=89.4$ °C, and $T_3=88.1$ °C indicate three transition temperatures. Three downward arrows labeled with numbers indicate three temperatures at which rotation data are obtained and shown in Fig. 2. The molecular structure of 8O23[7F8-] is shown at the top.

*Present address: Advanced Photon Source, Argonne National Laboratory, Argonne, IL 60439.

By acquiring the optical parameters Δ and Ψ with high-resolution null-transmission ellipsometry (NTE), molecular arrangements in free-standing films can be characterized. In our setup, Δ is the phase difference between $\hat{p}$ and $\hat{s}$ components of the incident light necessary to produce linearly polarized transmitted light, and Ψ describes the polarization angle of the output linearly polarized light. By putting eight equally spaced electrodes around the hole on a film plate, an in-plane rotatable E can be created. The azimuthal angle of E is denoted by α. Detailed description of our NTE can be found in recent papers [16,23].

Figures 1(a) and 1(b) show Δ and Ψ as a function of temperature from a ten-layer film upon cooling with $E=22$ V/cm and $E=8.9$ V/cm, respectively. With a large field ($E=22$ V/cm), three transitions can be identified at 90.8 °C (T_1), 89.4 °C (T_2), and 88.1 °C (T_3) in Fig. 1(a). Above T_1, the film is in the uniaxial Sm-A phase with no tilted surface layers. At T_1, surface layers begin to tilt. The parameter Δ acquired under $\alpha=90°$ (Δ_{90}) is different from Δ obtained under $\alpha=270°$ (Δ_{270}), so is Ψ. As temperature decreases further, around T_2, $\Delta_{90}-\Delta_{270}$ begins to decrease and $\Psi_{90}-\Psi_{270}$ continues to increase. At T_3, $\Delta_{90}-\Delta_{270}$ ($\Psi_{90}-\Psi_{270}$) suddenly increases (decreases). According to previous experimental results [10,16], such data suggest that an anticlinic structure forms between T_2 and T_3 and a synclinic structure forms below T_3. The structure between T_1 and T_2 is different from both synclinic and anticlinic structures. As it will be identified in the following, the structure between T_1 and T_2 is the nonplanar structure. The transition at T_2 seems to be continuous and different from the first order transition at T_3. When applied field is small ($E=8.9$ V/cm), there is a continuous transition happens at T_2 shown in Fig. 1(b). The structure below T_2 is synclinic. Between T_1 and T_2, the film has the nonplanar structure.

In order to get more detailed information and identify these three structures, rotations of E at different temperatures are performed. Such data at three typical temperatures with $E=22$ V/cm from a ten-layer film are given in Fig. 2. In this figure, (a), (b), and (c) show the data acquired at 90.5 °C, 89.2 °C, and 87.8 °C, respectively. A difference between these curves can be seen more clearly in Ψ versus Δ plots shown in Fig. 3. The curve for the synclinic structure has concave down and shows a wide span in Δ. The concave-right curve can be fit by an anticlinic structure [16]. For nonplanar structure, Ψ versus Δ plot does not show any clear concave and spans in Δ and Ψ are relatively small. Such plots demonstrate that surface layers form three distinct structures at these three temperatures.

To model these three surface structures, simulation of Δ and Ψ under rotations of E are conducted by using the 4×4 matrix method [24]. Each layer in the free-standing film is modeled as a uniaxial slab with extraordinary index of refraction n_e along $\hat{n}$ and ordinary index of refraction n_o along the other two principal axes. The indices of refraction and the layer spacing (d) are determined [16] by pulling a series of films at 93.5 °C where there are no tilted surface layers. Simulation are then implemented using measured values $n_e=1.499\pm0.002$, $n_o=1.417\pm0.002$, and $d=39.12\pm0.05$ Å. The simulation results are shown as solid lines in Figs. 2 and 3. Nonplanar, anticlinic, and synclinic structures are identified at 90.5 °C, 89.2 °C, and 87.8 °C, respectively. It confirms our suggestions of three structures from Fig. 1. To discuss these three structures, it is convenient to introduce the C director, which is the projection of $\hat{n}$ onto the layer plane. As shown in the diagrams in Fig. 3, two C directors of surface layers are parallel (azimuthal angle difference $\delta\phi=0°$) for synclinic structures and antiparallel ($\delta\phi=180°$) for anticlinic structures. Nonplanar structures have $\delta\phi\neq0°$ or 180°. For simplicity, only the two outermost surface layers are assumed to be tilted. From simulation results, the molecules in the two surface layers at 90.5 °C have $\delta\phi\approx90°$. The tilt angle of the surface layers determined by simulation in Fig. 3 from (a) to (c) is 5.6°, 6.8°, and 8.6°, respectively. The surface tilt angle increases upon cooling as expected [15].

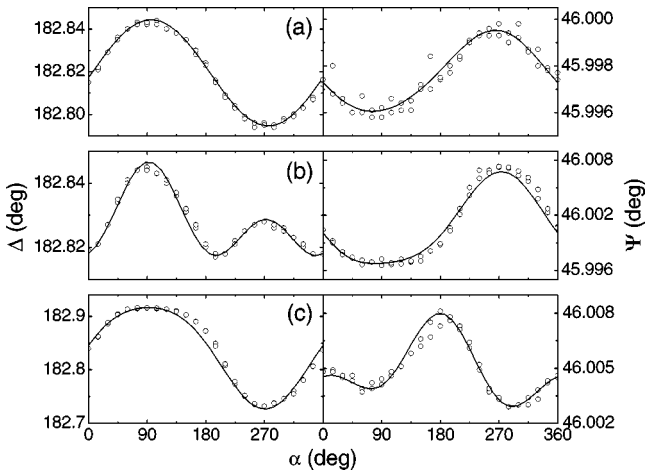

FIG. 2. Δ, Ψ versus α from a ten-layer film under $E=22$ V/cm. Data in (a), (b), and (c) are acquired at 90.5 °C, 89.2 °C and 87.8 °C that correspond to (1), (2), and (3) in Fig. 1 respectively. Symbols are data and the solid lines are simulation results.

The data in Fig. 1 suggest that the transition from the nonplanar to anticlinic [Fig. 1(a)] and from the nonplanar to

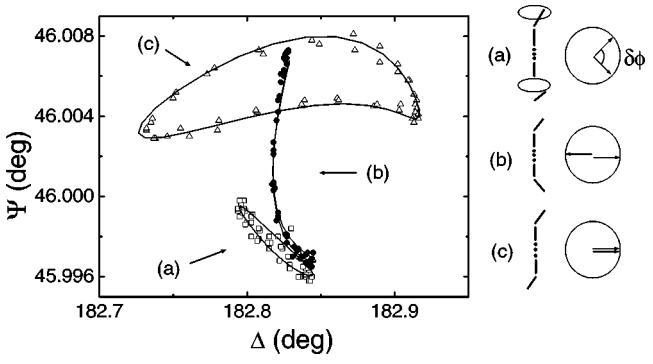

FIG. 3. Ψ versus Δ of the data and simulation results in Fig. 2. The solid lines are simulation results. The diagrams on the right-hand side show the corresponding tilt structures and arrangement of the C directors of the surface layers: (a) nonplanar, (b) anticlinic, and (c) synclinic.

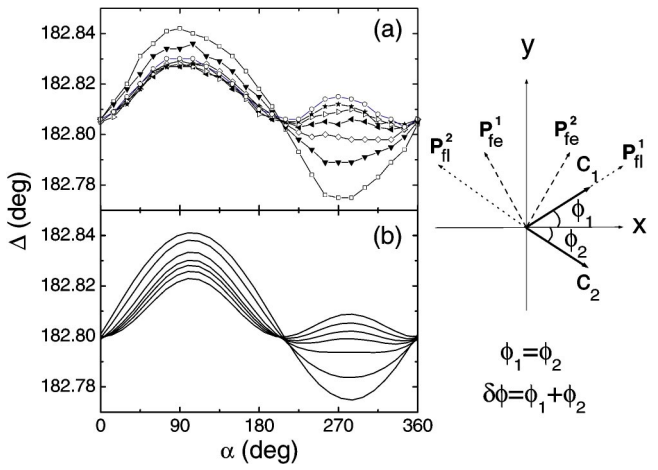

FIG. 4. (a) Δ as a function of α at different temperatures with $E=22$ V/cm. Different symbols are data at different temperatures, 90.3 °C (□), 90.1 °C (▼), 90.0 °C (◇), 89.9 °C (▲), 89.7 °C (▷), 89.6 °C (⋆), 89.4 °C (○). Solid lines are guides to the eye. (b) Simulation results with a model described in text. Seven curves have same tilt 7.5° and different $\delta\phi$ as 90°, 112°, 135°, 147°, 154°, 162°, and 171° from bottom to top for Δ_{270}. In the diagram, the xy-plane is the layer plane. C, P_{fe}, and P_{fl} are C directors, ferroelectric, and flexoelectric polarization, respectively. 1 and 2 represent two surface layers. E is in the y direction.

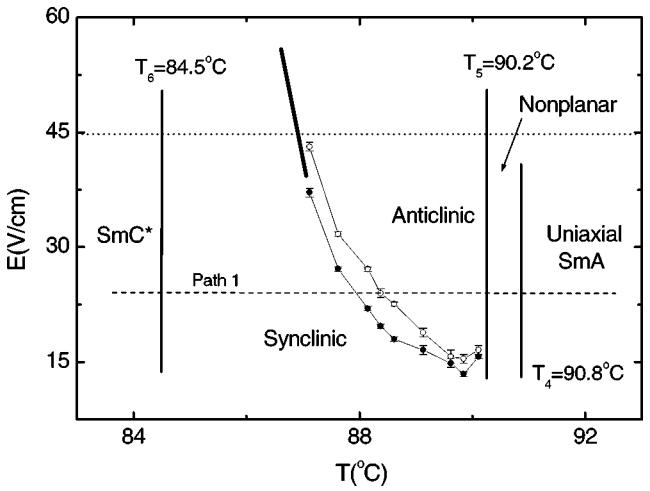

FIG. 5. Phase diagram for ten-layer films. Open and solid circles are results from ramping E up and down, respectively. Solid lines connecting symbols (above which molecules adopt an anticlinic structure) are guides to the eye. The three vertical solid lines at T_4, T_5, and T_6 separate four temperature windows. The heavy solid curve is an extrapolation of the boundary separating synclinic and anticlinic states. The dotted line at $\approx$45 V/cm indicates the maximum available E. The horizontal dash line shows the path of one temperature ramp.

synclinic [Fig. 1(b)] may be continuous. Between heating and cooling runs, no hysteresis is observed through these transitions within the experimental resolution. To strengthen this observation, under $E=22$ and 8.9 V/cm the Ψ and Δ versus α data were acquired with a small temperature increment (0.1 K). Some data obtained with $E=22$ V/cm are shown in Fig. 4(a). (Ψ is not shown to save space.) As we can see, Δ_{90} (Δ_{270}) continuously decreases (increases) as temperature decreases. This continuous evolution of Δ versus α as a function of temperature can be qualitatively described by the following picture. Due to chirality [25] ferroelectric polarization P_{fe} is perpendicular to the tilted plane, and flexoelectric polarization P_{fl} is along the tilt direction [26]. The vertical (along layer normal) component of P_{fl} of two surface layers cancels each other. As depicted in the diagram of Fig. 4, in the nonplanar state x components of P_{fe} of two surface layers cancel each other, so as P_{fl}. The effective polarization is along y (E) direction and comes from both P_{fe} and P_{fl}. As temperature decreases, the azimuth difference of two surface layers continuously increases to 180°. P_{fe} of two surface layers will cancel and P_{fl} becomes dominant. For comparison, simulation results are presented in Fig. 4(b) with the above picture. Here we assume that only two surface layers are tilted. The tilt angle keeps the same when $\delta\phi$ continuously increases from 90° to 171°. The simulations yield the similar curves as in Fig. 4(a). The continuous nonplanar-synclinic transition from our data obtained with $E=8.9$ V/cm can also be understood by the same approach, namely, the changes in contributions to the polarization.

By comparing the data in Figs. 1(a) and 1(b), it is obvious that increasing E can induce a transition from the synclinic to anticlinic structure. In order to explore the field and temperature dependence of the synclinic-anticlinic transition, E scans at different temperatures are performed for a ten-layer film. Temperature decreases with 0.25 K per step and at each step E is ramped up and down at $\alpha=270°$. From the jump of Δ or Ψ, the critical field E_c is found. The phase diagram is plotted in Fig. 5. Along Path 1 shown in Fig. 5, a nonplanar-anticlinic-synclinic transition is expected and observed as shown in Fig. 1(a). When E is below 13.7 V/cm, no anticlinic structure is observed and the rotation data show synclinic structure curves as in Fig. 2(c) [27].

Many films of 16 different thicknesses (N) have been studied. For thinner ones ($N<8$), results similar to Fig. 1(b) have been obtained and no anticlinic structures have been observed under the largest field available in our setup ($\simeq$45 V/cm). For thicker films ($N>8$), all three surface structures have been observed under appropriate fields. E_c which induces synclinic-anticlinic transition decreases as the film thickness increases. This thickness dependence of E_c is similar to the one in which increasing E can induce transition from anticlinic to synclinic [17].

Coupling between P_{fl} (P_{fe}) and E, which favors anticlinic (synclinic) arrangement is believed to be the main driving force in forming surface structures [18,19,28]. Upon increasing E, the anticlinic-synclinic transition has been reported by several groups [17,18]. Since at sufficiently large field all the molecules will tilt in the same orientation, it is understandable that the anticlinic-synclinic transition happens with increasing E. Rovšek *et al.* explained anticlinic-synclinic transition using a phenomenological model without considering flexoelectric polarization [29]. On the other hand, the synclinic-anticlinic transition is relatively rare. Because of synclinic-anticlinic transition happening at a small E_c, it is hard to believe E would change the tilt profile in

order to increase P_{fl} so that anticlinic structure is favorable.

Another interesting result is that the nonplanar structure forms near the onset of the surface transition. It does not form as an intermediate state between the anticlinic and synclinic states. This may be because the effective polarization will be largest if $\delta\phi$ between two surface layers is about 90° when P_{fl} and P_{fe} of two surface layers have approximately the same magnitude. As temperature decreases, surface layers will tilt more and P_{fe}, P_{fl} and elastic energy will change. Since the nonplanar structure costs more elastic energy, the film will either choose an anticlinic or a synclinic structure depending on E. So far, the nonplanar structure has only been observed in the NLS compounds. It is possible that this nonplanar structure is unique for this special group of compounds.

In conclusion, a nonplanar-anticlinic-synclinic or nonplanar-synclinic transition has been observed upon cooling. The transition from nonplanar to anticlinic (or synclinic) is found to be continuous. The changes in the contributions to the polarization are likely to be responsible for this continuous evolution. These new experimental results provide some guidance for the successive theory of these NLS liquid crystals.

This research was supported in part by the National Science Foundation, Solid State Chemistry Program, under Grant No. DMR-0106122 and by the donors of the Petroleum Research Fund, administered by the American Chemical Society. X.F.H. wishes to acknowledge financial support from the Stanwood Johnston Fellowship.

[1] M.D. Radcliffe, M.L. Brostrom, K.A. Epstein, A.G. Rappaport, B.N. Thomas, R. Shao, and N.A. Clark, Liq. Cryst. **26**, 789 (1999).

[2] F. Giesselmann, P. Zugenmaier, I. Dierking, S.T. Lagerwall, B. Stebler, M. Kašpar, V. Hamplová, and M. Glogarová, Phys. Rev. E **60**, 598 (1999).

[3] J.P.F. Lagerwall, F. Giesselmann, and M.D. Radcliffe, Phys. Rev. E **66**, 031703 (2002).

[4] N.A. Clark, T. Bellini, R.-F. Shao, D. Coleman, S. Bardon, D.R. Link, J.E. Maclennan, X.-H. Chen, M.D. Wand, D.M. Walba, P. Rudquist, and S.T. Lagerwall, Appl. Phys. Lett. **80**, 4097 (2002).

[5] M.S. Spector, P.A. Heiney, J. Naciri, B.T. Weslowski, D.B. Holt, and R. Shashidhar, Phys. Rev. E **61**, 1579 (2000).

[6] J.V. Selinger, P.J. Collings, and R. Shashidhar, Phys. Rev. E **64**, 061705 (2001).

[7] A. de Vries, Mol. Cryst. Liq. Cryst. Lett. **49**, 179 (1979).

[8] R.B. Meyer and R.A. Pelcovits, Phys. Rev. E **65**, 061704 (2002).

[9] C.Y. Young, R. Pindak, N.A. Clark, and R.B. Meyer, Phys. Rev. Lett. **40**, 773 (1978).

[10] Ch. Bahr and D. Fliegner, Phys. Rev. Lett. **70**, 1842 (1993).

[11] D.R. Link, J.E. Maclennan, and N.A. Clark, Phys. Rev. Lett. **77**, 2237 (1996).

[12] P.M. Johnson, D.A. Olson, S. Pankratz, T. Nguyen, J. Goodby, M. Hird, and C.C. Huang, Phys. Rev. Lett. **84**, 4870 (2000).

[13] Ch. Bahr, Int. J. Mod. Phys. B **8**, 3051 (1994).

[14] T. Stoebe and C.C. Huang, Int. J. Mod. Phys. B **9**, 2285 (1995).

[15] S. Heinekamp, R.A. Pelcovits, E. Fontes, E.Y. Chen, R. Pindak, and R.B. Meyer, Phys. Rev. Lett. **52**, 1017 (1984).

[16] P.M. Johnson, D.A. Olson, S. Pankratz, Ch. Bahr, J.W. Goodby, and C.C. Huang, Phys. Rev. E **62**, 8106 (2000).

[17] C.Y. Chao, C.R. Lo, P.J. Wu, Y.H. Liu, D.R. Link, J.E. Maclennan, N.A. Clark, M. Veum, C.C. Huang, and J.T. Ho, Phys. Rev. Lett. **86**, 4048 (2001).

[18] D.R. Link, G. Natale, N.A. Clark, J.E. Maclennan, M. Walsh, S.S. Keast, and M.E. Neubert, Phys. Rev. Lett. **82**, 2508 (1999).

[19] P.O. Andreeva, V.K. Dolganov, C. Gors, R. Fouret, and E.I. Kats, Phys. Rev. E **59**, 4143 (1999).

[20] D. Schlauf, Ch. Bahr, V.K. Dolganov, and J.W. Goodby, Eur. Phys. J. B **9**, 461 (1999).

[21] X.F. Han, D.A. Olson, A. Cady, D.R. Link, N.A. Clark, and C.C. Huang, Phys. Rev. E **66**, 040701 (2002).

[22] X.F. Han, S.T. Wang, A. Cady, M.D. Radcliffe, and C.C. Huang, Phys. Rev. Lett. **91**, 045501 (2003).

[23] D.A. Olson, X.F. Han, P.M. Johnson, A. Cady, and C.C. Huang, Liq. Cryst. **29**, 1521 (2002).

[24] D.W. Berreman, J. Opt. Soc. Am. **62**, 502 (1972); H. Wöhler, G. Haas, M. Fritsch, and D.A. Mlynski, J. Opt. Soc. Am. A **5**, 1554 (1988).

[25] R.B. Meyer, L. Liebert, I. Strzelecki, and P. Keller, J. Phys. (Paris), Lett. **36**, L69 (1975).

[26] Both Link's [18] and Andreeva's [19] description of P_{fl} give the same result here.

[27] Under very small field (0.2 V/cm), the nonplanar structure is observed, which is similar to that reported in Ref. [21].

[28] R.B. Meyer, Phys. Rev. Lett. **22**, 918 (1969).

[29] B. Rovšek, M. Čepič, and B. Žekš, Phys. Rev. E **66**, 051701 (2002).